Science Forum (Journal of Pure and Applied Sciences)

Journal Homepage: https://atbu.edu.ng/science-forum/

Physical Properties and Structural Analysis of Activated Carbon Produced from *Canarium schweinfurthii* Seed Using Phosphoric Acid as Activating agent and Its Application on Dye Effluent

Moshood Olayinka Ahmed[1], Doris Ezekiel Amin Boryo[2], Auwal Adamu Mahmoud[3]

[1]Medical Application Unit, Department of Radiological Safety, Nigerian Nuclear Regulatory Authority
[2]Department of Chemistry, Abubakar Tafawa Balewa University Bauchi, Nigeria
[3]Department of Chemistry, Abubakar Tafawa Balewa University Bauchi, Nigeria

ABSTRACT

Activated carbon was produced from Canarium schweinfurthii seed by physical and chemical processes. Phosphoric acid was used as an activating chemical at various concentrations (30 – 60%). The reaction conditions were optimized at a temperature range of 400 – 600 0C and a time interval of 20 – 60 minutes. The raw Canarium schweinfurthii seed and carbonized charcoal were characterized using parameters like bulk density, percentage yield, moisture content, ash content, and percentage of carbon. The uncarbonized Canarium schweinfurthii seed has a bulk density of 0.4348, percentage yield 93 %, moisture content 4.7 %, ash content 2.3 % and percentage of carbon 93 %, while the carbonized charcoal at temperature range of (400 – 600 0C) has a bulk density of (0.4115 – 0.4312 g/cm3), percentage yield (80.82 – 86.48 %), moisture content (13 – 17 %), ash content (6 – 2 %) and percentage of carbon of (74.005 – 84.510 %). The activated carbon was further used to decolourize dye effluent. The experimental data were analyzed using Langmuir, Freundlich and Temkin isotherms. After optimization, the activated carbon was structurally analyzed using Fourier-transform infrared spectroscopy (FTIR), Scanning electron microscope (SEM), Brunauer-Emmett-Teller (BET), and X-ray diffraction (XRD).

ARTICLE INFO

Received 28 December 2023
Received in Revised Form
11 January 2024
Accepted 11 January 2024
Published 20 February 2024
Available online 20 February 2024

KEYWORDS

Activated Carbon,
Phosphoric Acid
Canarium schweinfurthii

Corresponding Author: Moshood Olayinka Ahmed ✉ yinkusbabyonline@yahoo.com ✉ Medical Application Unit, Department of Radiological Safety, Nigerian Nuclear Regulatory Authority. © 2024 Faculty of Science, ATBU Bauchi. All rights reserved

Introduction

Activated carbon, also known as activated charcoal or activated coal is a form of carbon that has been processed tomake it extremely porous, thereby making it have a large surface area which can then be used for chemical reactions and adsorption (Harry and Francisco, 2006). Over the years, the use of activated carbon has evolved from medieval times to this modern day. Charcoal has been a household name for many centuries and thus its importance and usefulness cannot be overemphasized (Harry and Francisco, 2006). As a result of its importance in all life's endeavors, this has led to searching for various agricultural byproducts to produce activated carbon.

Most domestic and agricultural byproducts are biodegradable, but some of them take time before being degraded completely, hence constituting environmental nuisance. El-Sayed *et al.* (2014) said the production of activated carbon from agricultural byproducts has both economic and environmental effects, as it converts unwanted, low-value agricultural waste to useful high-value adsorbent. Agricultural waste products like shells, husks, seeds, pods, stems, and weeds are good sources of activated carbon production. Researchers have done extensive work on some agricultural byproducts like coconut shells, groundnut shells, and corn pods (El-Sayed *et al.,* 2014).

The research work aims to determine the physical properties and structural analysis of activated carbon produced from domestic wastes namely Canarium schweinfurthii seed with phosphoric acid as activating reagent.

Sampling and Analysis

Experimental Section

Canarium schweinfurthii (Atile) seed was sourced from the University roundabout near the University of Jos hostel, Jos, Plateau State Nigeria. 50 grams of pulverized *Canarium schweinfurthii* seeds were placed in jars containing 100 ml of Phosphoric acid with an impregnation ratio of 1:2, (IR 1:2). The jars were labelled appropriately as 30, 40, and 60 % phosphoric acid. After 24 hours, the *Canarium schweinfurthii* seed solution was decanted leaving behind a sludge. The sludge of *Canarium schweinfurthii* seeds was packed into crucibles and placed in the furnace. The reagent concentration ranged from 30 % to 60 %, the temperature of activation ranged from 400 ^{0}C to 600 ^{0}C as well as time of activation varied at 20-minute intervals from 20 to 60 minutes.

Proximate Analysis

Determination of Moisture content

1g of the sample was weighed and heated in a watch glass at 105 ^{0}C for 2 hours. The Heated crucible was cooled and re-weighed (Rafie, 2013).

Moisture percentage = (*Loss in weight on drying* (*g*))/ (*Initial weight* (*g*) *x* 100 (1)

Determination of Ash Content

3g sample was weighed and heated in open crucibles at 750 ^{0}C for 1.5 hours. The crucible was then cooled and re-weighed (Rafie, 2013).

Ash percentage= (Ash weight)/ (Oven dry weight) x 10 (2)

Determination of percentage yield of carbonized charcoal

Samples of bio-waste were dried weighed and carbonized in a furnace at 400 ^{0}C, 500 ^{0}C, and 600 ^{0}C for 1 hour. The charcoal product was weighed (Sumrit *et al.,* 2015).

The percentage yield was calculated as follows:

percentage yield = (*weight of raw material – weight of carbonized raw material*)/ (*weight of raw material*) *x* 100 (3)

Determination of Percentage of Carbon

Percentage of carbon in the raw material is determined by removing the Ash percentage and Moisture percentage from 100%.

percentage carbon = 100 – *Percentage ash – Percentage moisture* (4)

Determination of Bulk Density

A small quantity of charcoal carbonized at 400 ^{0}C, 500 ^{0}C, and 600 ^{0}C was taken and ground to powder; sieved, and separately put into the density bottle and weighed. The weight and

the volume of the density bottle had been initially determined. The bulk density was calculated using the following expression:

Bulk density=

(mass of carbon sample)/(volume)

(5)

Determination of Percentage Decolourization

Percentage decolourization was calculated using the following mathematical expression for each set of activated carbon and their effect on dye effluent:

$$percentage = (Do - D1)/Do \times 100$$

(6)

Where D_O = initial dye effluent absorbance

And D_1 = Final dye effluent absorbance after application of activated carbon overnight

Adsorption Isotherms

Freundlich, Langmuir, and Temkin isotherms were used to study the type of interaction between the prepared activated carbons and the dye effluent.

Freundlich Isotherm

This isotherm is an empirical equation and can be employed to describe heterogeneous systems.

Where: qe = Kf e1/n

(7)

Where qe is the amount of substance adsorbed at equilibrium in (mg/g), Ce is the equilibrium adsorbate concentration in the fluid (mg/L), 1/n is a heterogeneity factor less than 1 if the adsorption process is favorable, Kf is the Freundlich constant which is a measure of adsorption capacity (mg/g). KF can also be defined as the adsorption or distribution coefficient and represents the quantity adsorbed for a unit equilibrium concentration (Ashok, 2016). The linearized form of Freundlich model is given by the equation 2:

Log qe = log Kf + 1/n log Ce

(8)

A plot of log qe against log Ce gives a straight line with 1/n as slope and log Kf as intercept.

Langmuir Isotherm

The Langmuir isotherm assumes monolayer adsorption on a uniform surface with a finite number of adsorption sites. Once a site is filled, no further sorption can take place at that site. As such, the surface will eventually reach a saturation point where maximum adsorption at the surface is achieved (Saad *et al.,* 2008). The linear form of the Langmuir isotherm model is given by equation 10 and the separation factor by equation 3:

$$ce/qe = 1/(KL\ qm) + ce/qm$$

(9)

$$RL = 1/(1 + KL\ Co)$$

(10)

Where *C*e is the equilibrium concentration of the adsorbate (mg/L), *q*e is the amount adsorbed per unit mass of adsorbent (mg/g), *KL* is the Langmuir adsorption constant and *qmax* is the maximum adsorption capacity (mg /g). RL is a dimensionless constant referred to as a separation factor or equilibrium parameter. If RL > 1, the adsorption is unfavorable, RL = 1 it is linear, 0 < RL < 1 the adsorption is favorable and if RL = 0, the adsorption is irreversible.

Temkin Isotherm

The Temkin isotherm model contains a factor that explicitly takes into account the interactions between adsorbate and adsorbent species (Banerjee and Chattopadhyaya, 2013). It further implies that the heat of adsorption of all the molecules in the layer would decrease linearly with the coverage involved in this interaction. The linear form of the Temkin model is expressed as follows (Banerjee and Chattopadhyaya, 2013):

qe = B ln KT + B ln Ce

(11)

Where: B = RT/b

(12)

Where KT is the Temkin equilibrium binding constant (L/mg) corresponding to maximum binding energy and constant B is related to the heat of adsorption. The adsorption data were analyzed according to Equation 11. A plot of qe versus ln Ce yielded linear lines which enable the determination of the isotherm constants KT and

B from intercepts and slopes respectively (Banerjee and Chattopadhyaya, 2013).

Results and Discussions

Table 1 shows the physical properties of the raw material and the produced adsorbents. The lower ash content reveals that it is a useful candidate for adsorption. This assertion is agreed to by (Ismaila *et al.* 2016).

Table 1: Physical Properties of the Uncarbonized Canarium Schweinfurthii Seed

Physical Properties	Temperature (^{0}C)	Uncarbonized atile
Bulk density (g/cm3)		0.4348
Moisture content (Wt. %)		4.7
Ash content (Wt. %)		2.3
Percentage of Carbon (Wt. %)		93
Percentage yield (Wt. %)	400	86.48
	500	81.30
	600	80.82

Table 2: Physical Properties of the Carbonized Charcoal

Physical Properties	Temperature (^{0}C)	Carbonized Atile
Bulk density (g/cm3)	400	0.4115
	500	0.4299
	600	0.4312
Moisture content (Wt. %)	400	19.945
	500	15.907
	600	13.49
Ash content (Wt. %)	400	6
	500	2
	600	2
Percentage of Carbon (Wt. %)	400	74.055
	500	82.093
	600	84.510

The bulk density of the raw material is 0.4348 g/cm^3, ash content 2.3%, moisture content 4.3%, carbon content 93%, and percentage yields of the charcoal are 80.82%, 81.3%, and 86.48 at 400 ^{0}C, 500 ^{0}C and 600 ^{0}C respectively.

Effect of Carbonization on Bulk Density

The bulk densities as indicated in Tables 1 and 2 above showed no significant difference as would have been expected. However, the bulk density of the raw *Canarium schweinfurthii* in Table 1 was 0.4348 g/cm^3 which is higher than the carbonized *Canarium schweinfurthii* in Table 2. This observation supports the claim of Ekebafe *et al.* (2017), which states that, at high heating temperatures, the bulk density reduces which may be due to the opening of the interstitial spaces (microspores) in the carbon residue.

Effect of Carbonization Ash Content

From the Table, the determined ash contents are 2.3 % for the raw material. While after

carbonization the ash content was determined as 6 % at 400 ^{0}C, 2 % at 500 ^{0}C, and 2 % at 600 ^{0}C. The charcoal's ash content varies from 0.5 % to more than 5 % depending on raw materials. Good quality charcoal typically has an ash content of around 3 %, (Harry 2019).

Effect of carbonization moisture content

The moisture content of the raw material is 4.7 %, however, that of the carbonized materials ranged from 13 – 29 %. The high moisture content of carbonized raw material could be a result adsorption of moisture. When charcoal is freshly prepared, the moisture content is around 1%. However, when charcoal is left over time, the hygroscopicity is increased, hence moisture content of charcoal can rise to 15 % or even more (Harry 2019).

Effect of Carbonization on Percentage Yield

The percentage yield as seen in Table 1 above indicated a reduction in yield with an increase in temperature from 86.48 at 400 ^{0}C to 80.82 at 600 ^{0}C. The rate of weight loss is primarily due to the initial large number of volatiles that can be easily released with increasing temperature as well as the loss of moisture to a lesser extent (Eric *et al.,* 2014).

Effect of carbonization on the percentage of carbon

From the Table above (Table 1), the percentage of carbon increases with increasing temperature simply because the ash, moisture, and volatile contents have reduced at those high temperatures. This observation is supported by Harry (2019), and according to Ukrainian biofuel suppliers, the fixed carbon content of charcoal ranges from a low of about 50% to a high or around 95%.

Table 3: pH of the Optimized Activated Carbons

S/N	Activated Carbon	pH
1	E9	5.1
2	F4	5.8
3	G7	4.1
4	H6	5.0

Percentage Decolourization

The calculated percentage decolourization of the optimized samples is illustrated in Fig 1 below.

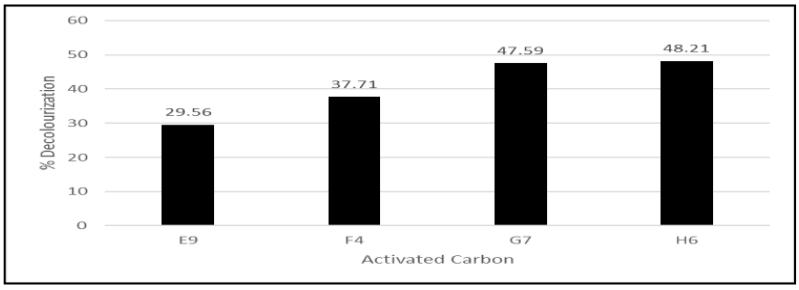


Figure 1: Optimum Conditions of Activate Carbon for Percentage Decolourization

E9-------30% phosphoric acid activated carbon at 600 ^{o}C for 60 minutes
F4-------40% phosphoric acid activated carbon at 500 ^{o}C for 20 minutes
G7-------50% phosphoric acid activated carbon at 600 ^{o}C for 20 minutes
H6-------60% phosphoric acid activated carbon at 500 ^{o}C for 60 minutes

Surface Morphology

The micrograph of prepared activated carbons is presented in Figures (2 - 5) respectively. These figures showed cavities, pores, and rough surfaces. The surfaces are pitted and fragmented due to carbonization and activation using chemical methods (Ismaila *et al.* 2016).

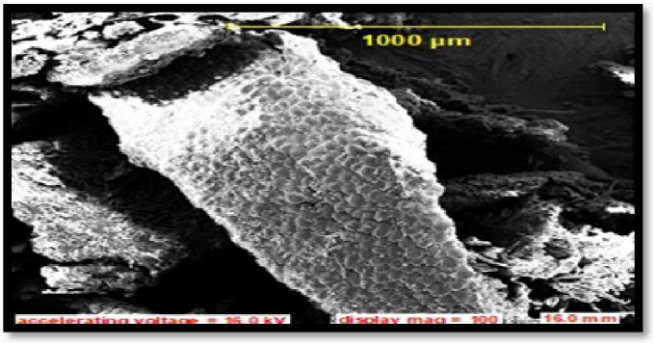


Figure 2: SEM Micrograph of Raw Canarium Schweinfurthii (Mag = 100)

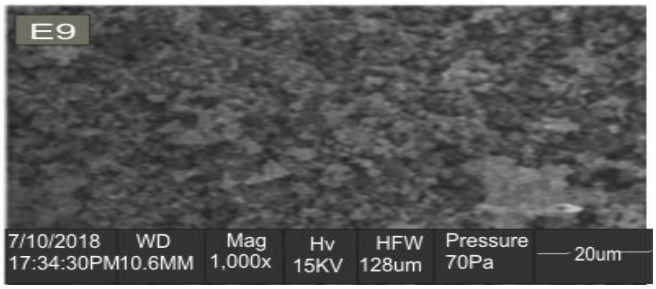


Figure 3: SEM Micrograph of ActivatedCarbon E9 (Mag = 1,000)

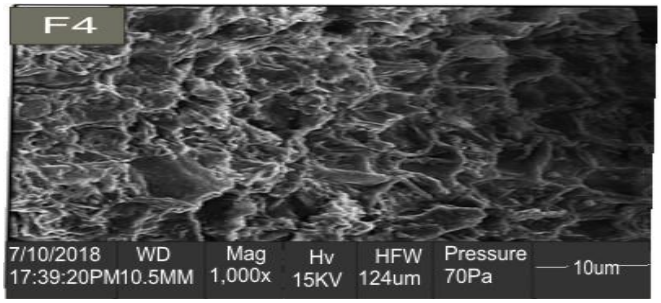


Figure 4: SEM Micrograph of ActivatedCarbon F4 (Mag = 1,000)

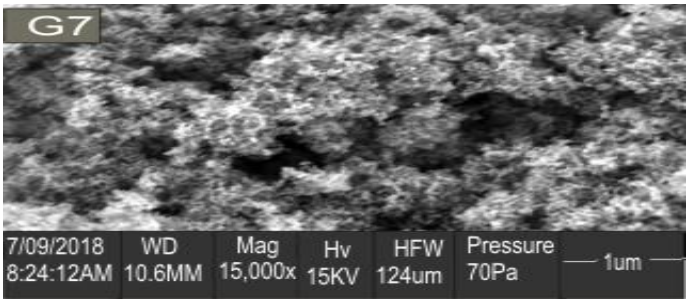


Figure 5: SEM Micrograph Of ActivatedCarbon G7 (Mag = 15,000)

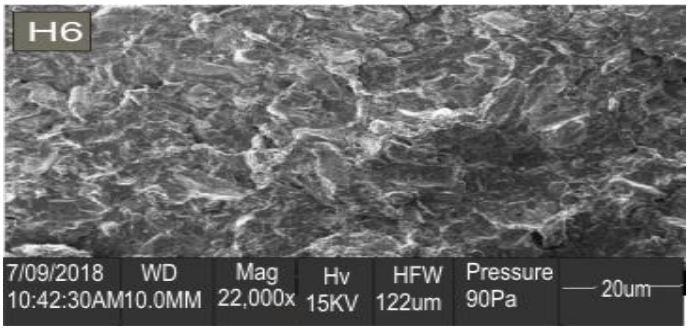


Figure 6: SEM Micrograph of Activated Carbon H6 (mag = 22,000)

Surface Area and Pore Characteristics

G7 (Fig1) showed some narrow pores on its surface which are formed when the precursor materials are subjectedto heat treatment at the appropriate temperature and conditions (Solum *et al.*1995) and (Bacher 2002).

G7 and H6 micrographs reveal morphological characteristics of the surface of the prepared activated carbon showing structures having cavities, pores, and rough surfaces (Tan and Hameed, 2017). In addition, there are remarkable changes in the external surfaces with quite irregular cavities and pores which is also observed by Hesas *et al*. (2013) in the surface morphology of the activated carbon produced from apples, however, these irregular pores are non-existent the raw apple.

Table 4: Physical Properties of Carbonized Atile (E9 and F4) Using Brunauer-Emmett-Teller (BET)

E9		F4	
Temperature (T/^{0}C)	Specific Surface Area (m^2/g)	Temperature (T/^{0}C)	Specific Surface Area (m^2/g)
100	1036.86	100	945.30
200	1032.13	200	960.21
300	1100.50	300	990.30
400	1021.34	400	915.10
500	1001.43	500	912.20
600	1034.88	600	910.02
Mean	1037.86		938.86

Table 5: Physical Properties of Carbonized Atile (G7 and H6) Using Brunauer-Emmett-Teller (BET)

G7		H6	
Temperature (T/^{0}C)	Specific Surface Area (m^2/g)	Temperature (T/^{0}C)	Specific Surface Area (m^2/g)
100	915.33	100	1020.60
200	900.21	200	1013.23
300	927.30	300	1350.00
400	910.10	400	1021.42
500	912.20	500	1020.22
600	816.42	600	1010.10
Mean	896.93		1072.6

Effect of Carbonization on Canarium Schweinfurthii Using Brunauer-Emmett-Teller (BET)

E9 activated carbon has an average surface area of 1037.86 m2/g, F4 is 938.86 m2/g, while G7 and H6 have mean surface areas of 896.93 and 1072.6 m2/g respectively. All these figures show high surface areas.

Functional Groups

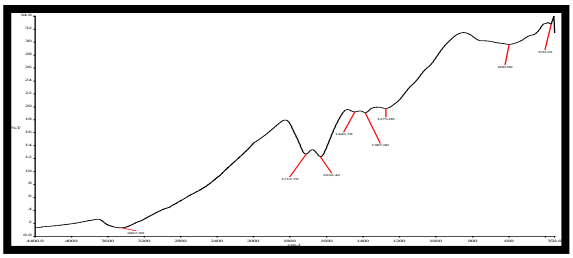


Figure 7: FTIR Spectra of E9

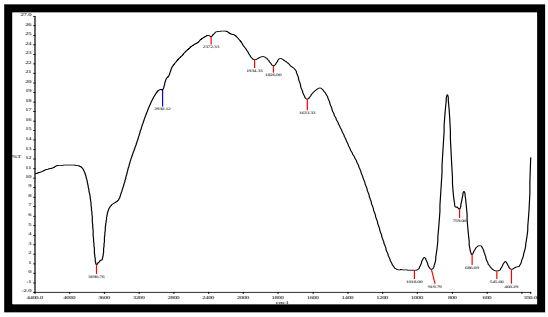


Figure 8: FTIR Spectra of F4

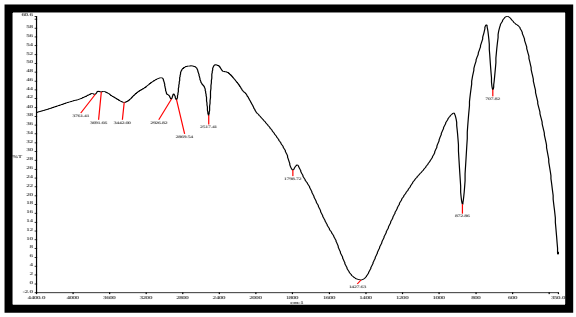


Figure 9: FTIR Spectra Of G7

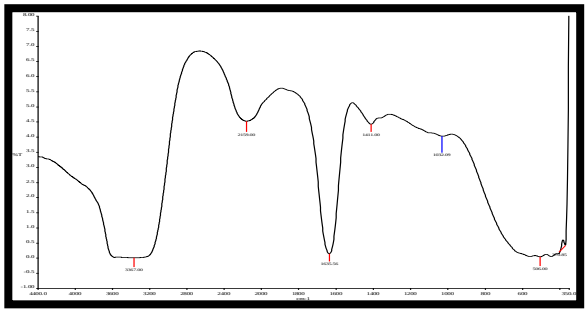


Figure 10: FTIR Spectra of H6

Infrared spectroscopy provides information on the chemical structure of the carbon material. Fig. (7-10) shows FTIR spectra of the synthetic carbons obtained by phosphoric acid activation at different concentrations (E9- H6). activated carbons G7 and H6 obtained by phosphoric acid activation at different concentrations. Observed Spectra: 3442 cm^{-1}: G7 (50 % phosphoric acid activated carbon at 600 ^{o}C for 20 minutes) and 3390 cm^{-1}: H6 (60 % phosphoric acid activated carbon at 500 ^{o}C for 60 minutes). This band can be assigned to the O–H stretching mode of hydroxyl groups. The position and asymmetry of this band at lower wave numbers indicated the presence of strong hydrogen bonds (from carboxyls, phenols or alcohols) (Solum *et al.,* 1995).

Samples G7 and H6 shows absorption bands due to saturated aliphatic C-H bands SP^3 at 2926.82 and 2918.00 cm^{-1} respectively. The small band 1798.72 cm^{-1} at G7 is assigned to C=O stretching vibrations of carboxylic acid, amide, and ketones (Zawadzki, 1989).

In H6, the band at 1040.00 cm^{-1} is usually found with oxidized carbons and has been assigned to C–O stretching which could be that of acids, alcohols, phenols, ethers and/or esters groups (Abdulkhalil *et al.,* 2013)

Adsorption Isotherms

Freundlich, Langmuir and Temkin isotherms were used to study the type of interaction between the prepared activated carbons and the dye effluent. Based on the values of experimental data using Langmuir, Freundlich and Temkin isotherms. The best correlation coefficients are, in increasing order of Freundlich models < Temkin model < Langmuir model. Therefore, it could be concluded that the data best fit is Langmuir adsorption model since it has the highest individual value of 0.9989.

Freundlich Isotherm

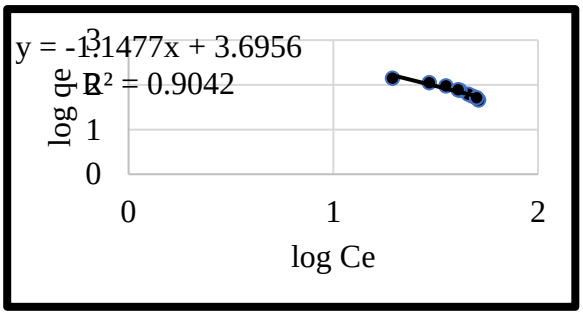


Figure 11: Freundlich Isotherm of E1-E9

Key 1:

E1--- 30 % phosphoric acid activated carbon at 400 ^{0}C for 20 minutes, E2---30 % phosphoric acid activated carbon at 400 ^{0}C for 40 minutes, E3---30 % phosphoric acid activated carbon at 400 ^{0}C for 60 minutes, E4---30 % phosphoric acid activated carbon at 500 ^{0}C for 20 minutes, E5---30 % phosphoric acid activated carbon at 500 ^{0}C for 40 minutes, E6---30 % phosphoric acid activated carbon at 500 ^{0}C for 60 minutes, E7---30 % phosphoric acid activated carbon at 600 ^{0}C for 20 minutes, E8---30 % phosphoric acid activated carbon at 600 ^{0}C for 40 minutes, E9---30 % phosphoric acid activated carbon at 600 ^{0}C for 60 minutes.

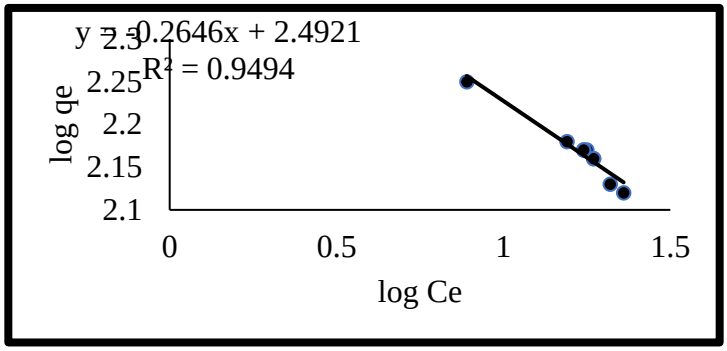


Figure 12: Freundlich Isotherm of F1-F9

Key 2:
F1--- 40 % phosphoric acid activated carbon at 400 ^{0}C for 20 minutes, F2---40 % phosphoric acid activated carbon at 400 ^{0}C for 40 minutes, F3---40 % phosphoric acid activated carbon at 400 ^{0}C for 60 minutes, F4---40 % phosphoric acid activated carbon at 500 ^{0}C for 20 minutes, F5---40 % phosphoric acid activated carbon at 500 ^{0}C for 40 minutes, F6---40 % phosphoric acid activated carbon at 500^{0}c for 60 minutes, F7---40 % phosphoric acid activated carbon a 600 ^{0}C for 20 minutes, F8---40 % phosphoric acid activated carbon at 600 ^{0}C for 40 minutes, F9---40 % phosphoric acid activated carbon at 600 ^{0}C for 60 minutes.

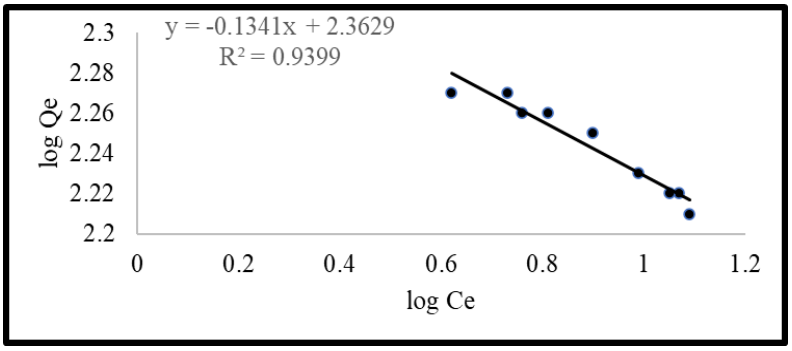


Figure 13: Freundlich Isotherm of G1-G9
Key 3:
G1--- 50% phosphoric acid activated carbon at 400^{0}c for 20 minutes, G2---50% phosphoric acid activated carbon at 400^{0}c for 40 minutes, G3---50% phosphoric acid activated carbon at 400^{0}c for 60 minutes, G4---50% phosphoric acid activated carbon at 500^{0}c for 20 minutes, G5---50% phosphoric acid activated carbon at 500^{0}c for 40 minutes, G6---50% phosphoric acid activated carbon at 500^{0}c for 60 minutes, G7---50% phosphoric acid activated carbon at 600^{0}c for 20 minutes, G8---50% phosphoric acid activated carbon at 600^{0}c for 40 minutes, G9---50% phosphoric acid activated carbon at 600^{0}c for 60 minutes.

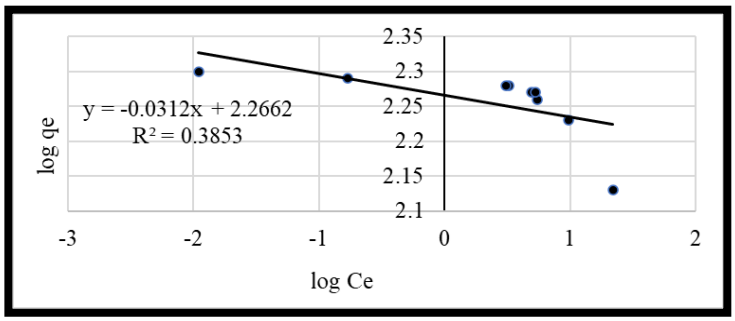


Figure 14: Freundlich Isotherm of H1-H9

Key 4:

H1--- 60% phosphoric acid activated carbon at 400^{0}c for 20 minutes, H2---60% phosphoric acid activated carbon at 400^{0}c for 40 minutes, H3---60% phosphoric acid activated carbon at 400^{0}c for 60 minutes, H4---60% phosphoric acid activated carbon at 500^{0}c for 20 minutes, H5---60% phosphoric acid activated carbon at 500^{0}c for 40 minutes, H6---60% phosphoric acid activated carbon at 500^{0}c for 60 minutes, H7---60% phosphoric acid activated carbon at 600^{0}c for 20 minutes, H8---60% phosphoric acid activated carbon at 600^{0}c for 40 minutes, H9---60% phosphoric acid activated carbon at 600^{0}c for 60 minutes.

Temkin Isotherm

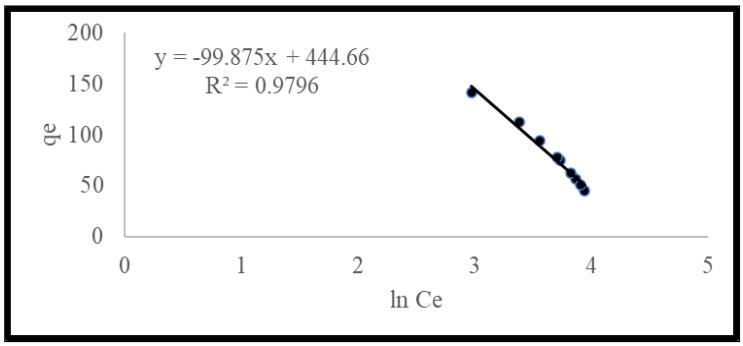


Figure 15: Temkin Isotherm of E1-E9

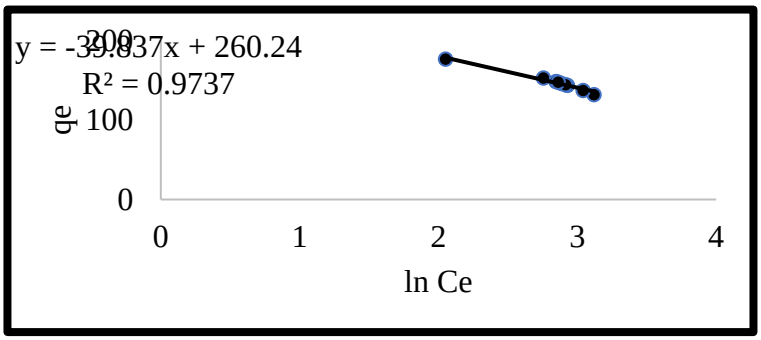


Figure 16: Temkin Isotherm of F1-F9

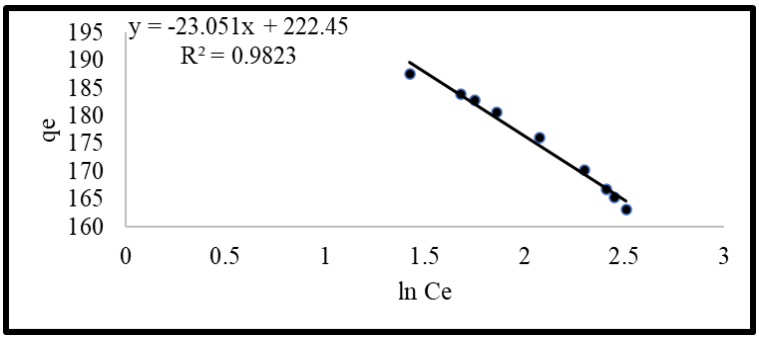


Figure 17: Temkin Isotherm of G1-G9

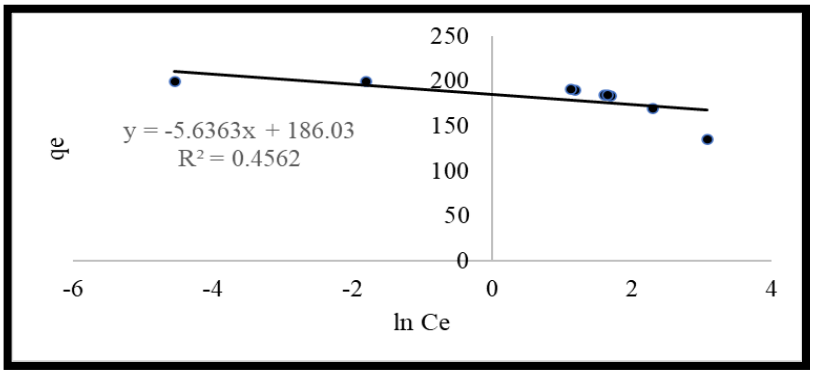


Figure 18: Temkin Isotherm of H1-H9

Langmuir Isotherm

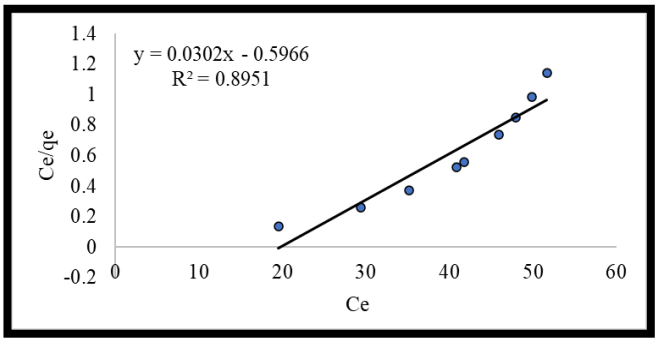


Figure 19: Langmuir

Isotherm of E1-E9

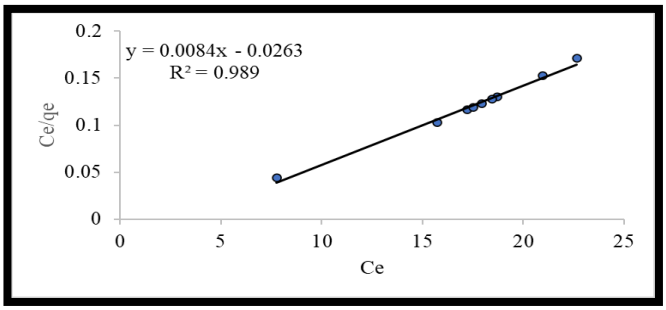


Figure 20: Langmuir Isotherm of F1-F9

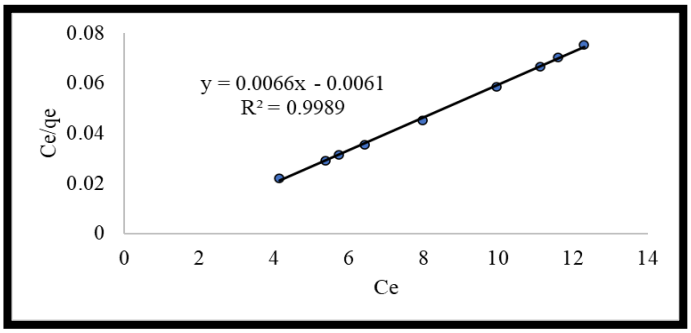


Figure 21: Langmuir Isotherm of G1-G9

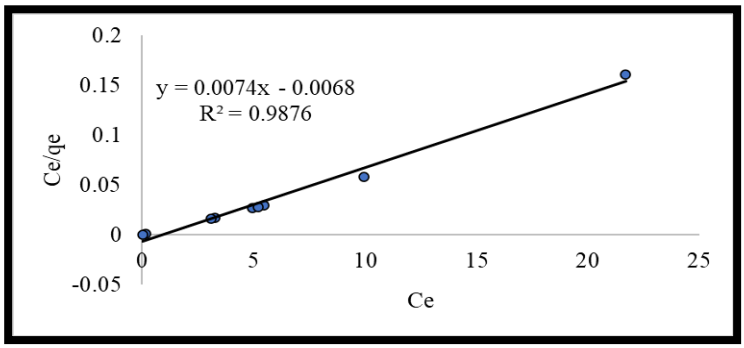


Figure 21: Langmuir Isotherm of H1-H9

X-Ray Diffraction Patterns

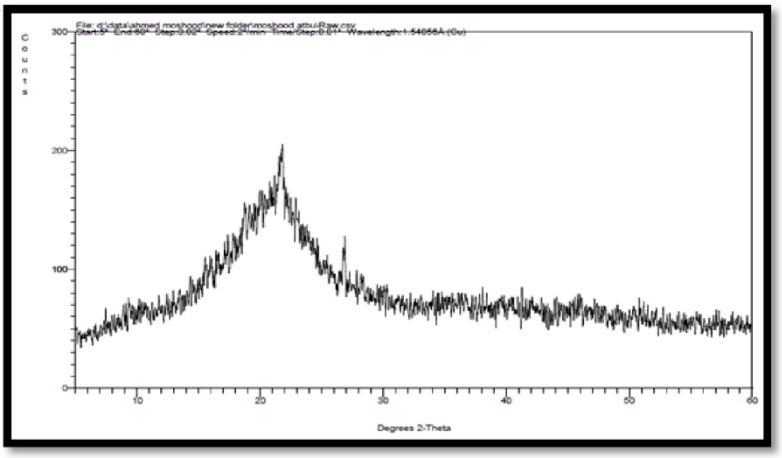


Figure 22: X-Ray Diffraction of Raw Canarium Schwienfurthii

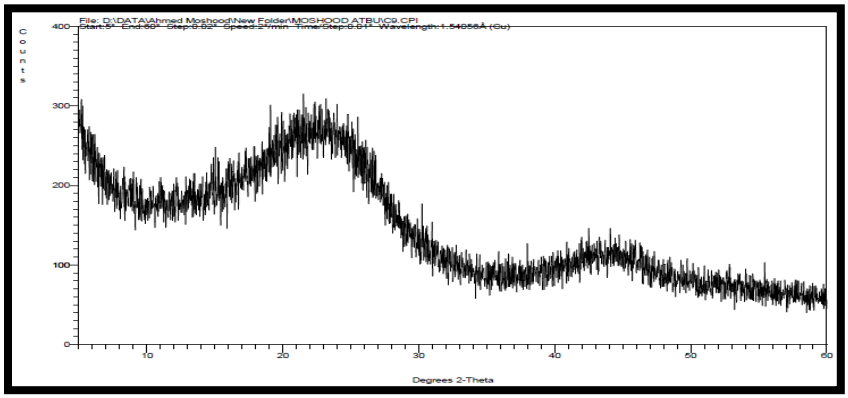


Figure 23: X-Ray Diffraction of Activated Carbon H6

Figure 22 depicts the XRD pattern of H6 (activated carbon formed by the 60 % H_3PO_4 activation at 500 °C for 60 minutes). It is characterized by the appearance of a broad diffraction background and the absence of characteristic sharp peaks. There are two broad halo diffraction backgrounds corresponding to 2 Θ = 24°, 45° in the spectrum. The spectrum shows the activated carbon is majorly amorphous and similar results have been reported for activated carbon produced from lignocellulosic raw material similar to what was obtained by Abdulkhalil *et al.* (2013).

Conclusion and Recommendation

The research work showed great results as all optimized activated carbon samples showed great characteristics as observed in the literature of other researchers. The SEM of all samples at different magnifications showed the presence of pores. The BET of the samples showed an average range of 896.93 – 1072.6 m2/g. These surface areas made these activated carbons a good candidate for adsorption. The FTIR analysis was also used to determine the presence of functional groups and the presence of common functional groups like O-H, C-O, C-H, C-C, and C=O were observed.

The adsorption isotherms analysis showed that the adsorption of dye effluent onto the prepared activated carbons fitted more into Langmuir and Temkin Isotherm and less into Freundlich isotherm.

This research recommends the use of *Canarium schweinfurthii* as a carbon source and phosphoric acid as an activating agent. In addition, this novel activated carbon could be employed in adsorption processes like heavy metal remediation in water and soil samples.

References

Abdulkhalil H. P. S., Jawaid M., Firoozian P., Rashid U., Islam A., and Akil5 H. M. 2013. Activated Carbon from Various Agricultural Wastes by Chemical Activation with KOH: Preparation and Characterization. *Journal of Biobased Materials and Bioenergy* 7: 1–7

Bacher A. (2002). Infrared spectroscopy handout. Retrieved on January 10, 2020 from www.chem.ucla.edu/~bacher/spectrocopy/IR1.html

Banerjee S. and Chattopadhyaya M. C. (2013). Adsorption characteristics for the removal of a toxic dye, tartrazine from aqueous solutions by a low cost agricultural by-product. Arabian Journal of Chemistry 10: S1629–S1638

Ekebafe L.O., Imanaha J.E., and Okieimen F.E. (2017). Effect of carbonization on the processing characteristics of rubber seed shell. *Arabian journal of chemistry.* 10: S174- S178

El-Sayed G. O., Yehia M. M., and Asaad A. A. (2014). Assessment of activated carbon Prepared from corncob by chemical activation with

phosphoric acid. *Journal of Water Resources and Industry*, **7** (8): 66–75

Eric M., Isaac O., and Askwar H. (2014). Preparation of activated carbon with desired properties through optimization of impregnating agent. *Research Journal in Engineering and Applied Sciences* **3** (5): 327-331

Freundlich, H. K. (1909). Academishe Bibliotek: Leipzig

Harry B. (2019). Food and agricultural organization of the United Nations. Manual on making charcoal 'The quality of charcoal'. Retrieved on June 18, 2019 from http://www.fao.org/3/x5328e/x5328e0b.htm.

Harry M., and Francisco Rodriguez-Reinoso F. (2006). **Textbook of Activated Carbon**. New York, Elsevier Science and Technology Books. (1): 9-22

Hesas H. R., Aramiya-Niya A., Daud W. M., and Sahu J. N. (2013). Activated carbon adsorbent. BioResources journal. 8 (2): 2950-2966

Ismaila O. A., Folahan A. A. and Gabriel A. O. (2016). Adsorption of p-Phenylenediamine onto activated carbon prepared from Jatropha curcas and Terminalia catappa seed coats. Jordan journal of chemistry. 11 (1): 50 – 67

Rafie, R. M. (2013). Waste lubricating oil treatment by extraction and adsorption. *International Refereed Journal of Engineering and Science*. (2): 1-11

Saad, S. M., Awwad N. S. and Aboterika H. A. (2008). *The Journal of Hazardous Material*. 154: 992– 997.

Solum M.S., Pugmire R.J., Jagtoyen M. and Derbyshire F. (1995). Evolution of carbon structure in chemically activated wood. *Journal of Carbon*. **33**: 1247-1254

Solum M.S., Pugmire R.J., Jagtoyen M. and Derbyshire F. (1995). Evolution of carbon structure in chemically activated wood. Journal of Carbon. 33: 1247-1254

Sumrit M., Phansiri M., Wanwimon P., and Sataporn Khumpai (2015). The *Scientific World Journal*. 2015: 1-9.

Tan K.L. and Hameed B.H. (2017) Insight into the adsorption kinetics models for the removal of contaminants from aqueous solutions. Journal of the Taiwan Institute of Chemical Engineers 7 (4): 25–48

Zawadzki J. (1989). Infrared spectroscopy in surface chemistry of carbons. P.A. Thrower (Ed.), Chemistry and Physics of Carbon textbook. Marcel Dekker Ltd., New York, pp. 147-386